

Electronic phenomena in the conducting phases of orientationally disordered fullerides

E.J. Mele, S.C. Erwin, M.S. Deshpande

Department of Physics, Laboratory for Research on the Structure of Matter, University of Pennsylvania, Philadelphia, PA 19104, USA

Received 4 November 1993; accepted 21 January 1994

Abstract

A review of recent theoretical work describing three-dimensional electron propagation in the orientationally disordered fullerides is presented. We discuss some of the experimental consequences of on-site orientational disorder for the conducting state, and highlight parallels between the physics of the doped fullerides and of the conducting polymers.

Keywords: Electronic phenomena; Fullerides; Conducting phases

1. Introduction

The alkali-doped fullerides provide a new class of molecular metals which have attracted the attention of physicists, chemists and materials scientists over the last two years [1,2]. These are fascinating systems from both a structural and electronic point of view. In this paper we will briefly review our theoretical work on the electronic phenomena in the conducting phases of the fullerides [4–6], and highlight several parallels between the physics of the conducting doped polymers and that of the doped fullerides.

At the outset, it is important to recognize that in both classes of materials one is dealing with ‘molecular metals’ and a key issue is therefore the nature of the three-dimensional charge transport in an intrinsically low-dimensional host. Thus, the electronic structure of the doped polymers is dominantly one dimensional, and in the fullerides it is zero dimensional, yet the solid state properties are quite strongly affected by the weak intermolecular interactions which determine the three-dimensional nature of the composite. For the doped fullerides this is now known to depend in an essential way on the orientational structure of the host. Here we will discuss a theory of this system which treats this interaction between the orientational degree of freedom and the electronic properties. We note that orientational phase transitions are also known to occur

in the alkali-doped polymers, and these are likely to play an important role in determining the three-dimensional electronic behavior there as well. Additionally, there are striking spectroscopic signatures in the doped states which are also common to both systems, and we will comment on this aspect of the physics towards the end of the paper.

2. Orientational disorder

The conducting phases M_xC_{60} with $x=3$ and $M=(K, Rb)$ have attracted the most attention because they exhibit superconducting ground states, with surprisingly high transition temperatures [1]. Structurally, these solids can be described as orientational glasses [7]. The C_{60} molecules are located on the lattice sites of a close-packed face-centered cubic Bravais lattice, with the alkali saturating the high symmetry octahedral and tetrahedral interstitial sites. Below a crossover temperature of approximately 166 K [8], the rotational dynamics of the C_{60} slows dramatically, so that at low temperatures the negatively charged fullerenes lock into a high symmetry setting in the cubic crystal field of the cations. This setting aligns the two-fold axes of the molecule along the (001) axes of the crystal. However, there are two inequivalent ways in which the C_{60} can achieve this setting, which are related by a $\pi/2$ rotation

about any (001) direction. This rotation is not a symmetry operation of the molecule and, thus, the two high symmetry settings are structurally inequivalent.

It is now recognized that on-site orientational disorder in this form has an enormous effect on almost all the electronic properties of the conducting phases. To understand why, we notice that although the π electron manifold of the C_{60} spans an energy of order 10 eV, the conduction band for the doped carriers is only of order 0.5 eV wide, and is derived from an antibonding t_{1u} state of the isolated molecule. This state transforms as a vector under spatial rotations, much like an atomic 'p state'. The conduction bandwidth is then controlled by the relatively weak intermolecular hopping amplitudes between these t_{1u} molecular orbitals on neighboring C_{60} units. These are extraordinarily sensitive to the relative orientation of neighboring molecules owing to the vector nature of the conduction band state, the antibonding character of the state and the fact that the intermolecular amplitudes are inevitably dominated by the carbon sites of closest approach along a given bond direction [9].

The sensitivity of the intermolecular hopping amplitude on molecular orientation can be understood by looking at the contact between two C_{60} units along a nearest-neighbor (110) direction on the f.c.c. lattice. This is shown in Fig. 1 for two neighboring molecules in the 'A' orientation, and for the contact between orthogonal (i.e. A and B) settings. In either case, one finds that the '5–6' bond is eclipsed in the two configurations. However, the relative orientations of the nearest five-fold and six-fold rings are reversed. Since the relevant frontier t_{1u} orbital is antibonding in character, this implies that reorientation of the molecule effectively reverses the sign of the hopping amplitude for this orbital. This is tantamount to inverting the top and bottom of the t_{1u} -derived conduction band so that the energy scale of the disorder is of the order of the Fermi energy for the doped carriers.

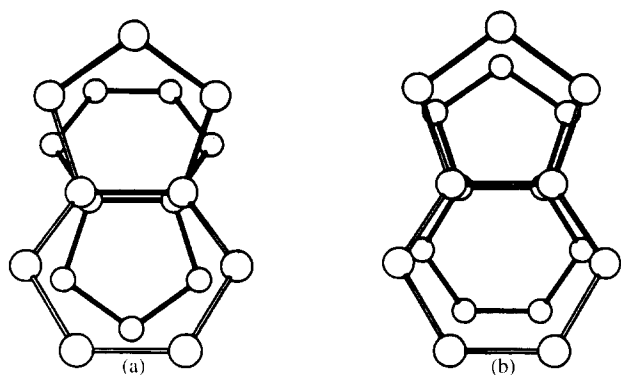


Fig. 1. Atomic configurations along a nearest-neighbor (110) bond for two fullerenes in the AA orientation (a) and in the AB orientation (b).

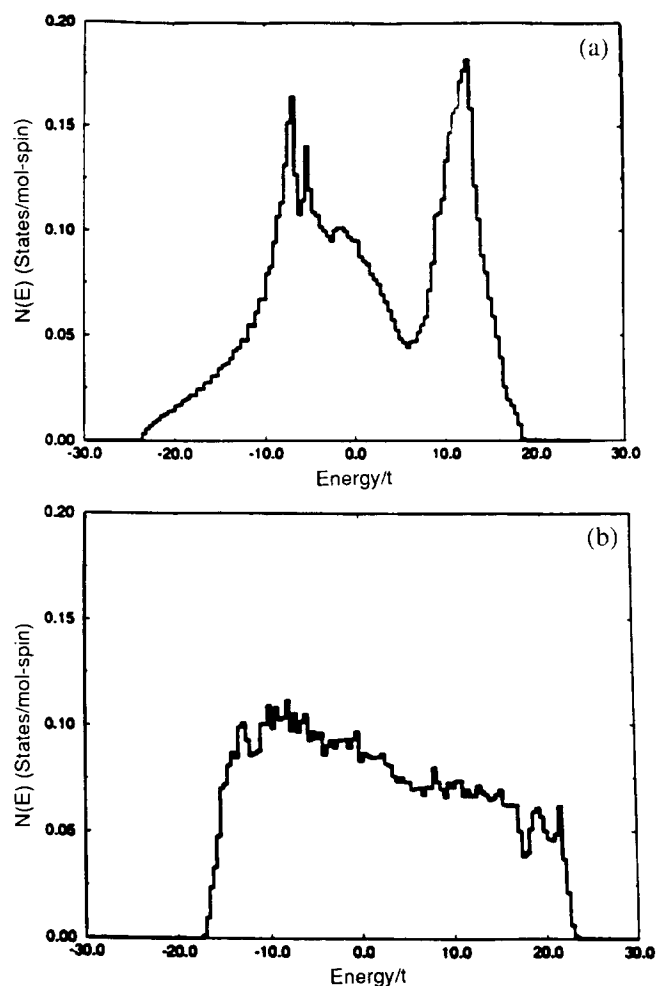


Fig. 2. Conduction band density of states for the ordered unidirectional crystal (a), and for the fully disordered quenched alloy (b). The energy scale parameter t is approximately 10 meV.

The effects of this orientational disorder on the electronic structure in the t_{1u} conduction band are therefore very strong. As an example, in Fig. 2, we compare the k -integrated density of states for the fully orientationally ordered structure (so-called unidirectional structure with all the molecules in the standard A orientation) and in a supercell with quenched uncorrelated on-site orientational disorder (here the sites are randomly assigned to the A and B orientations). One observes that the sharp structure in the density of states of the ordered phase is 'washed out' in the disordered phase, leaving a broad and structureless continuum in the t_{1u} conduction band [3,9].

3. Gauge model for the disordered state

The arguments given in section 2 about the effect of orientational disorder on the electron propagation in the conduction band overlook an essential aspect of the physics. There it was argued that a reorientation

of neighboring molecules can induce a sign change, that is a phase shift of π , for a particle propagating across a nearest-neighbor bond between C_{60} units with orthogonal settings. Of course, this idea posits that we work in a basis in which the t_{1u} molecular orbitals are rigidly fixed in the molecular frame, so that they co-rotate with the reoriented molecule. If instead, we adopt a convention in which the t_{1u} basis states are fixed in the crystal frame, there is no difference in phase for an electron traversing an AA bond, and an AB bond along the (110) direction. To state this dilemma more precisely, we cannot meaningfully discuss the phase accumulated by a particle propagating along any single bond of the network since this is not a gauge invariant quantity. Instead, we need to examine the total ‘phase’ accumulated on a closed electron trajectory on the lattice, a quantity which is invariant under local gauge transformations. Furthermore, the local gauge transformations relevant to this problem are not the simple $U(1)$ rotations as suggested above, but rather the full set of 3×3 orthogonal transformations within the t_{1u} orbital basis.

Our model for electron propagation in the doped fulleride is summarized in the diagram in Fig. 3 [3]. Starting from a reference site (shown as the bold dot) and a reference orbital polarization (shown as the arrow on this site), the effect of the hopping Hamiltonian is to transport the electron to a neighboring site and to reorient its orbital moment. After completion of a closed trajectory on the lattice, one finds that the particle has undergone a net reorientation of its orbital moment, returning to the origin with a new orbital polarization given by the dashed arrow. This reorientation depends on the specific electron trajectory, so that a different path, though possibly containing the same number of steps, generally yields a different reorientation of the reference orbital polarization as shown schematically in Fig. 3(b).

The density of states in such a model is obtained from a trace of the single-particle Green’s function, in which one sums over all such closed paths, traces over orbital polarizations, and ensemble averages over the possible molecular orientations. It is important to identify the effective length, ξ , over which the orbital polarization of our test particle remains correlated on its trajectory after such an average. One knows that for the orientationally ordered crystal, this correlation length diverges, so that the Green’s function remains sensitive to the very largest closed loops which can be constructed within a macroscopic sample. The sharp structure in the density of states of Fig. 2(a) originates from the constructive interference from precisely these extensive loops in the crystal.

By contrast the smooth structure in Fig. 2(b) indicates that the correlation length is finite, and possibly quite short for this phase. To address this question more

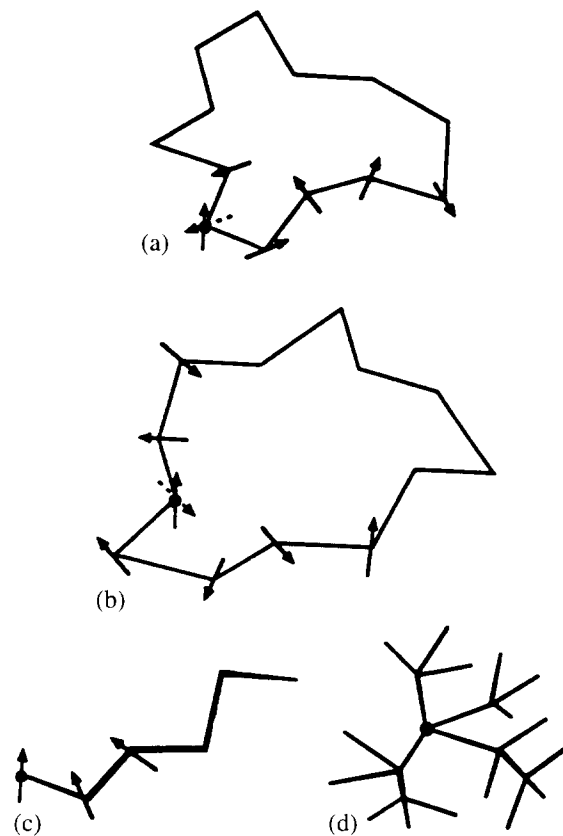


Fig. 3. Electron trajectories which contribute to the single-particle Green’s function. (a) and (b) Two inequivalent 13-step trajectories which yield different reorientations of the electron orbital moment. (c) Retraceable path which dominates the asymptotic behavior of the Green’s function in the disordered medium. (d) Tree which allows only retracing paths.

quantitatively, we consider a theoretical model in which the effective orbital dephasing length is set to zero. In such a system, after the ensemble average, closed loops of finite area cannot contribute to spectral weight in the one-particle Green’s function. Instead, the asymptotic structure of the single-particle Green’s function is dominated by the elementary retracing paths, in which an electron propagates away from our reference site, and returns along exactly the same path. A full three-dimensional network in which these retracing paths are patched together has the topology of a Cayley tree or Bethe lattice, with one and only one path connecting any two distant nodes of the network. In Fig. 3(d) a model for such a tree is shown with coordination $n=4$. In our calculations for the fullerides, we consider an effective medium with coordination number $n=12$, which retains the local coordination and symmetry of the full f.c.c. network. Each bond in our three-band Bethe lattice then describes a real nearest neighbor 3×3 matrix hopping amplitude along a particular oriented bond in this structure [3].

The density of states calculated for the fulleride tree is shown in Fig. 4. Here we observe a broad and

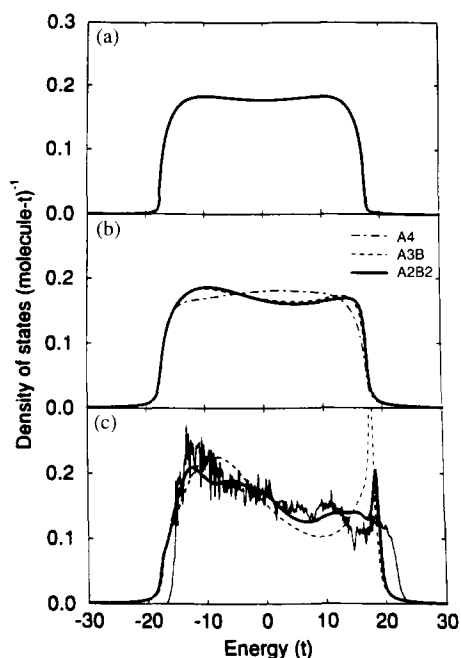


Fig. 4. Density of states for the fulleride tree (a) is compared with the density of states obtained by embedding molecular clusters inside the effective medium. (b) The cluster is a regular tetrahedron excised from the f.c.c. lattice (four sites which are mutually nearest neighbors). (c) The cluster is closed to include the (200) and (211) coordination shells. The noisy curve is the result of an ensemble average over many cells containing quenched orientational disorder.

structureless continuum, reflecting the absence of closed coordination rings on the network. This spectrum is also an even function of energy, an exact symmetry property of this model [3,6]. Remarkably, the overall bandwidth obtained in this calculation is very nearly the bandwidth obtained from full numerical simulations on disordered lattice models, reflecting the fact that the asymptotic structure of the Green's function in the disordered medium is indeed controlled by the retracing Brinkman–Rice paths [10].

However, in contrast to the tree model for the disordered fulleride, numerical simulations on disordered fulleride lattices reveal a pronounced and systematic asymmetry in the conduction band density of states, with the spectral weight enhanced at negative energies in the conduction band. As an example, the noisy curve in Fig. 4(c) presents the results of an ensemble average of the Green's functions over many supercells (typically 100 models each containing 27 molecules are taken in the average) with quenched orientational disorder, and this spectrum shows exactly this effect. This asymmetry is the result of the residual phase coherent propagation of the electrons in closed loops of finite area on the disordered lattice. To demonstrate the effect, we have constructed a model which retains the lowest order closed loops, by excising a regular tetrahedron from the full f.c.c. lattice and embedding this cluster within the effective disordered

medium, treated in the tree approximation developed above. One finds that for any of the tetrahedral clusters which contain unlike molecular orientations, spectral weight is indeed enhanced at negative energies. This is nevertheless a very weak effect for a cluster of this size as seen in Fig. 4(b), and the Green's function remains dominated by the strong orbital dephasing due to coupling of the cluster to the disordered external network.

By carrying out similar calculations in which both the size and symmetry of the embedded cluster are varied, one is able to probe quantitatively the development of correlations in the orbital polarization for a particle propagating in the disordered medium [3]. One finds that the cluster+tree models converge suitably to the lattice simulations, but only after a phase coherent propagation through relatively large rings are accounted for in the theory. To illustrate, in Fig. 4(c), we present results in which closed rings through the (200) and (211) coordination shells are retained in the calculations. One finds that even these larger clusters are contributing significantly to the observed asymmetry of the conduction band. One concludes that the effective electronic correlation length in the disordered phase is rather longer than initially expected, and is estimated to lie in the range of 20–25 Å. The physics is that only for closed rings of this size does the constructive interference among the various low order closed lattice trajectories begin to compete with the very strong orbital dephasing induced by coupling the cluster to the external medium.

4. Experimental consequences

In this section we will briefly review some of the consequences of the model developed in section 3. The implications of this model are far reaching and several have direct parallels in the physics of the conducting polymers. A number of the experimental implications of this model for the fullerenes are still being explored [5,6].

The effective mean free path deduced in section 3 is surprisingly large. We note that the Fermi wavevector in these systems is approximately 0.5 \AA^{-1} , and so that $k_F \xi$ is of order 10!. This is surprisingly large in view of the absence of prominent structure in the k -integrated spectral functions of Fig. 2. The result suggests that a decomposition in the Green's function in momentum space can provide a way to expose some of the structure which remains hidden in the k -integrated spectra of Fig. 2.

To illustrate the effect, in Fig. 5, we display the single-particle momentum distributions at the Fermi energy for four different structural models [6]: (a) the reference fully orientationally ordered uni-directional

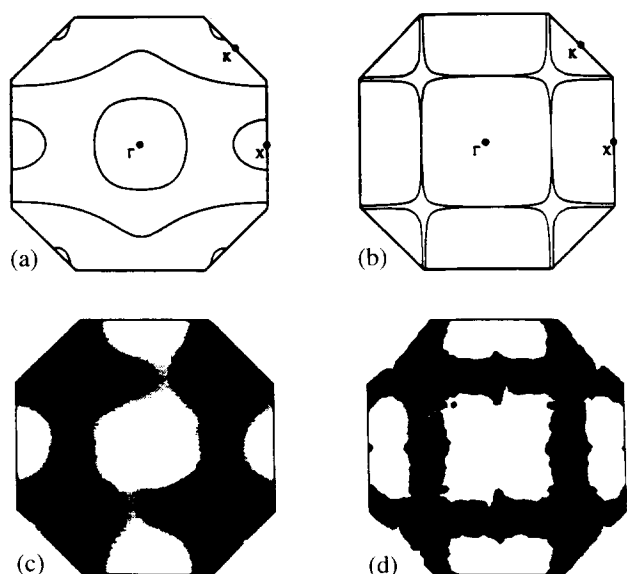


Fig. 5. Momentum distributions on the Fermi energy for four different structural models: (a) orientationally ordered uni-directional structure; (b) virtual crystal in which the ensemble average is applied to the Hamiltonian; (c) cluster+tree model of the disordered phase; (d) numerical simulations on lattice models with quenched disorder. The Fermi surfaces show a correlation length of order 20 Å, and the symmetry is quite different from the ordered crystal, though described quite well by a disorder-broadened virtual crystal.

structure; (b) the result for an ordered virtual crystal (where the ensemble average is applied to the Hamiltonian before calculation of the Green's function [11]); (c) the cluster+tree model; (d) the result of numerical simulations on large disordered supercells (a numerical experiment). One sees, as expected, that the orientationally ordered phase provides a poor description of the situation for the various disordered models. In the disordered models we recover a pseudo C_4 symmetry of the full cubic crystal, and exhibit a disorder broadened 'Fermi surface' due to the finite correlation length. In fact, the orientational correlation length can be read directly from the widths of the momentum distributions in the second row of Fig. 5, confirming our earlier estimate in the range 20–25 Å.

The structure of the residual Fermi surface in these compounds is that of pairs of broadened but essentially flat two-dimensional sheets, normal to each of the (001) directions in k -space, which then intersect in lines along the (110) directions (with three-fold intersections at points along the (111) directions) as shown. This is precisely the topology of the sharp Fermi surface obtained for the virtual crystal which is shown in Fig. 5(b). This correspondence is remarkably robust, not only in the location, topology and symmetry of the Fermi surface, but also in the variation of the orbital polarization of the conduction states with 'angle' on the Fermi surface. Thus, the orientational disorder in this system is not sufficient to remove the effects of crystalline anisotropy in these metals. Overall, the spec-

tral functions for the disordered state are described quite well by a disorder broadened version of the virtual crystal.

In Fig. 6, we display the real (absorptive) part of the frequency-dependent conductivity through the mid-infrared, calculated for the uni-directional ordered crystal and for the orientationally disordered structure. For the ordered crystal we observe a strong Drude pole and a broad mid-infrared continuum which extends from $\omega=0$ –0.3 eV. The Drude pole in this model exhausts approximately 30% of the spectral weight from the conduction charge [5]. The effect of disorder is to broaden this Drude pole and to suppress the inter- t_{1u} continuum to lower energies. In the resulting spectrum it is difficult to unfold these two separate contributions in frequency, and the sum resembles a very soft and strongly overdamped peak with a non-Drude lineshape. One finds that it is nevertheless possible to decompose these two contributions to $\text{Re } \sigma$ by a separation of the short range (bound charge) and long range 'hydrodynamic' contribution to the full nonlocal conductivity $\text{Re } \sigma(x, x'; \omega)$ [3].

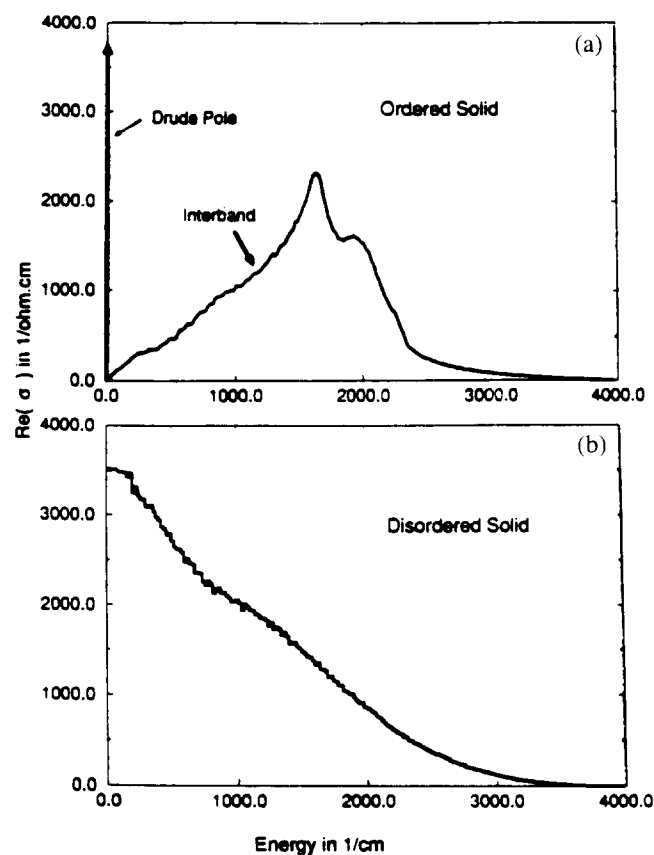


Fig. 6. Theoretically calculated $\text{Re } \sigma(\omega)$ is compared for the orientationally ordered uni-directional structure (a) and the disordered phase (b). Disorder broadens the Drude peak, and pulls the mid-infrared peak to lower energy. Experimental spectra show, in addition to an overdamped mid-infrared peak, modulation from the even-parity intramolecular vibrations.

The frequency-dependent conductivity through the mid-infrared has now been measured by several groups [12–14]. In the most careful of such measurements carried out in the normal state, one finds that the smooth and broad mid-infrared continuum is modulated by interference with the various even-parity intramolecular vibrations. This interference phenomenon is strictly forbidden in any inversion symmetric structure and it therefore directly probes the local breakdown of inversion symmetry due to the rotational disorder in the doped phase. The effect also turns out to depend sensitively on the precise electron–phonon coupling amplitudes [5], and a direct comparison between theory and experiment is then able to distinguish between several of the very popular interaction models which have been proposed to describe the doped fullerides [15,16].

The theory of this interference phenomenon is familiar from the physics of the doped polymers, and even of the charge transfer salts. One finds that the one-loop polarization corrections from the doped conduction charge renormalize both the frequencies and lifetimes of the intramolecular modes. This indirect interaction also provides a channel for coupling the various modes to a long wavelength dipole probe. The theory of the anomalous infrared active vibrational (IRAV) modes of doped polyacetylene [17] thus finds a direct analog and application in the doped fullerides. A more detailed account of this result and comparison with experimental data is in preparation [5].

On-site orientational disorder also has an important effect on the superconducting states of these doped systems. On a superficial level this appears to contradict Anderson's theorem, which maintains that for any disorder which preserves time-reversal symmetry, pairing between time-reversed eigenstates of the one-electron Hamiltonian is unaffected [18]. The physics of our problem seems more closely related to the observations of Ma and Lee [19] who some years ago suggested that in strongly disordered metals one could produce a 'localized superconductor'. This is an interesting state of matter which would exhibit the long wavelength electromagnetic properties of a conventional superconductor, but for which the Bogoliubov quasi-particle excitations are localized over a characteristic correlation length.

To study quantitatively the interplay of orientational disorder and the pairing dynamics in this problem we have constructed and solved a self-consistent Bogoliubov mean-field theory on a number of orientationally mixed lattice models [20]. This study reveals that the on-site rotational disorder will generally induce a modest degree of gap anisotropy into the quasi-particle spectra for the equilibrium low temperature paired states. This is a fascinating result because it violates the 'conventional wisdom' which would suggest that any intrinsic an-

isotropy in the pairing field will tend to be suppressed by the disorder. However, as we emphasized above, the effects of orientational disorder are rather subtle in this problem, and the crystal-field effects are robust in the electronic spectra calculated in the various disordered models. The resulting gap anisotropy leads to an apparent smearing of the gap edges, and a substantial band tailing into the effective 'gap' calculated for the paired phase. This in turn implies that the threshold for quasi-particle pair creation and the peaks in the k -integrated quasi-particle spectra for the paired state will occur at quite different energies. We find, after correcting for the trivial secular variation of the densities of states among various disordered models, that both the critical temperatures and gaps are renormalized downward by the rotational disorder [20]. The renormalization to the critical temperature is the stronger of the two effects, so that even within a weak coupling theory the reduced gap $2\Delta/kT_c$ is substantially enhanced relative to the BCS value of 3.53. Our calculations on various ordered short-period alloys typically yield an enhanced gap ratio in the range 3.8–4.0.

A survey of existing experimental data on the superconducting state reveals a variety of anomalous results which can be explained by strong coupling effects and/or strong gap anisotropy (two prominent examples are given in Refs. [21] and [22]). Both of these features fall outside the existing 'standard model' for the superconducting fullerides, which now needs to be developed further for these very interesting conducting phases.

5. Conclusions and summary

The doped fullerides provide yet another example of a composite intercalation system with novel structural and electronic properties. Here, we have emphasized the aspects of the theory which focus on the physics of three-dimensional electron propagation in a low-dimensional host. This is a subtle and quite fascinating problem which is quite commonly encountered in the conducting phases of the doped conjugated polymers, as well as in other molecular metals. As we have seen, these effects can play a dominant role in determining the macroscopic electronic behavior of these systems. As these effects are better cataloged and understood, improved control of the electronic properties in a wide class of molecular metals will hopefully follow.

Acknowledgements

This work was supported by the Department of Energy under Grant No. 91 ER 45118 and by the National Science Foundation under Grant No. 91 20668.

References

- [1] A.F. Hebard, *Phys. Today*, **45** (1992) 26.
- [2] J.E. Fischer and P.A. Heiney, Order and disorder in fullerene and fulleride solids, *J. Chem. Phys. Solids*, (Dec.) (1993).
- [3] M.S. Deshpande, S.C. Erwin, S. Hong and E.J. Mele, *Phys. Rev. Lett.*, **71** (1993) 2619.
- [4] M.J. Rice, H.-Y. Choi, E.J. Mele and M.S. Deshpande, *Phys. Rev. B*, **49** (1994) 3687.
- [5] M.S. Deshpande, E.J. Mele, M.J. Rice and H.-Y. Choi, (1994) in preparation.
- [6] E.J. Mele and S.C. Erwin, Electron propagation in orientationally disordered fullerenes, Preprint, 1993.
- [7] P. Stephens et al., *Nature*, **351** (1991) 632.
- [8] S.E. Barrett and R. Tycko, *Phys. Rev. Lett.*, **69** (1992) 3754.
- [9] M.P. Gelfand and J.P. Lu, *Phys. Rev. Lett.*, **68** (1992) 1050.
- [10] W.F. Brinkman and T.M. Rice, *Phys. Rev. B*, **2** (1970) 1324.
- [11] T. Yildirim, S. Hong, A.B. Harris and E.J. Mele, *Phys. Rev. B*, **48** (1993) 12 262.
- [12] L.D. Rotter, Z. Schesinger, J.P. McCauley, N. Coustel, J.E. Fischer and A.B. Smith III, *Nature*, **355** (1992) 532.
- [13] L. DeGeorgi, P. Wachter, G. Gruner, S.-M. Huang, J. Wiley and R.B. Kaner, *Phys. Rev. Lett.*, **69** (1992) 2987.
- [14] T. Pichler, M. Matus and H. Kuzmany, *Solid State Commun.*, **86** (1993) 221.
- [15] M. Schluter, M. Lannoo, M. Needels, G. Baraff and D. Tomanek, *Phys. Rev. Lett.*, **68** (1992) 526.
- [16] C.M. Varma, J. Zaanen and K. Ragavachari, *Science*, **254** (1991) 989.
- [17] E.J. Mele and M.J. Rice, *Phys. Rev. Lett.*, **45** (1980) 926.
- [18] P.W. Anderson, *Phys. Rev.*, **109** (1958) 1492.
- [19] M. Ma and P. Lee, *Phys. Rev. B*, **32** (1985) 5658.
- [20] S. Hong, S.C. Erwin and E.J. Mele, 1993, unpublished results.
- [21] A striking result for the spin relaxation rate $1/T_1$ is given in R. Kiefl et al., *Phys. Rev. Lett.*, **70** (1993) 3987.
- [22] Z. Zhang, C. Chen and C.M. Lieber, *Science*, **254** (1991) 1619.